In situ XAFS analysis of Pd–Pt catalysts during hydrotreatment of model oil

Kyoko K. Bando [a,*], Toshihide Kawai [b], Kiyotaka Asakura [c], Takashi Matsui [a], Lionel Le Bihan [a], Hiroyuki Yasuda [a], Yuji Yoshimura [a], S. Ted Oyama [d]

[a] *National Institute of Advanced Industrial Science and Technology, Tsukuba, Ibaraki 305-8569, Japan*
[b] *SPring-8, Japan Synchrotron Radiation Research Institute, Hyogo 679-5198, Japan*
[c] *Catalysis Research Center, Hokkaido University, Hokkaido 001-0021, Japan*
[d] *Virginia Polytechnic Institute and State University, Virginia 24061-0211, USA*

Abstract

Supported Pd–Pt catalysts are efficient for hydrodesulfurization (HDS) and hydrodearomatization (HDA) reactions of diesel fuel and their activity varied with the kinds of supports. Concerning HDA, alumina supported catalysts showed four times higher TOF (turn over frequency) than silica supported one. In order to elucidate the difference in activity, the structural analysis of the active phase was performed. After reduction pretreatment, relatively uniform and large metallic alloy Pd–Pt particles were formed on SiO_2, whereas, Pd and Pt atoms formed rather segregated particles on Al_2O_3. Subsequent X-ray absorption of fine structure (XAFS) analysis under HDS conditions showed no contribution of sulfur for SiO_2 supported catalyst, whereas, formation of sulfided metal species was observed in XAFS spectra for the Al_2O_3 supported catalyst. It is suggested that on Pd–Pt/SiO_2, thin sulfide layer on the metal cluster surface blocked the active sites and lowered the HDA activity. Presence of partially sulfided phase originated from rather segregated structure like Pd–Pt/Al_2O_3 is thought to be requisite for high HDA activity.
© 2005 Elsevier B.V. All rights reserved.

Keywords: In situ XAFS; Hydrodearomatization; Hydrodesulfurization; Pd–Pt; Model oil

1. Introduction

Supported Pd–Pt catalysts are known as efficient catalysts for both hydordesulfurization (HDS) and hydrodearomatization (HDA) of diesel oil [1,2]. However, either the precise mechanism or the structure of an active phase has not been clarified yet. It is reported that the HDA activity of the Pd–Pt catalysts greatly depends on the kinds of supports [3]. In our previous work, an in situ X-ray absorption fine structure (XAFS) analysis of Pd–Pt catalysts supported on SiO_2, Al_2O_3 and ultra stable Y-type zeolite (USY) was carried out and it was found that after activation by H_2 reduction, relatively uniform Pd–Pt metal particles were formed on SiO_2, whereas, on Al_2O_3 and USY, Pd and Pt atoms formed segregated fine particles [4]. The difference in catalytic activity among these catalysts was deeply related to the structure of the active phase. In the present

work, we focused on the SiO_2 and Al_2O_3 supported catalysts and performed in situ XAFS analysis of Pd–Pt catalysts under high pressure and high temperature liquid phase HDS conditions in order to elucidate the structure of an active phase under real reaction conditions.

2. Experimental

Supported Pd–Pt (molar ratio of Pd/Pt was 4) catalysts were prepared by impregnation method. Alumina (Catalysts and Chemicals Industry) and silica (Fuji Silysia Chemical) were used as supports. The precursors for Pd and Pt were $Pd(NH_3)_4Cl_2 \cdot xH_2O$ and $Pt(NH_3)_4Cl_2 \cdot xH_2O$, respectively. The total metal content was 2 wt.%. The impregnated samples were dried in vacuum at 333 K for 6 h, then calcined at 573 K under oxygen for 3 h.

In situ XAFS measurements were carried out at BL7C, 9A and 10 B of the Photon Factory in the Institute of Materials Structure Science, High Energy Accelerator Research Organization (PF-IMSS-KEK) in Japan. All the spectra were obtained in transmission mode. A flow reaction system

including an in situ XAFS cell [5] was assembled at the end of X-ray beam line. All the reaction conditions like temperature, pressure and a gas flow rate could be monitored and controlled from outside of the radiation shield room.

The sample was initially reduced at 573 K for 1 h under a flow of H_2. The flow rate was 50 cm^3/min. After reduction, the reactor was cooled to 553 K under H_2 and pressurized up to 4 MPa. Then a model oil composed of dibenzothiophene (DBT, sulfur = 500 ppm), tetraline (20 wt.%) and hexadecane (as a solvent) was introduced at a flow rate of 4 g/h with H_2 (the flow rate was set at 40 ml/min). The reaction condition was kept for 24 h.

XAFS spectra were observed under the reaction conditions every 10 min in a step-scanning mode. Analysis of extended X-ray absorption fine structure (EXAFS) and X-ray absorption near edge structure (XANES) data was conducted with commercially available software (REX, Rigaku Co.). Parameters for backscattering amplitudes and phase shift functions were extracted from the oscillations of standard substances (Pd foil, Pt foil, Pd–Pt alloy foil, PdS and PtS_2) observed at reaction temperatures in order to exclude influence of thermal oscillations at higher temperature from analysis, or they are created by FEFF8 (Washington University).

3. Results and discussion

3.1. Catalytic tests

Catalytic tests were performed for Pd–Pt/SiO_2 and Pd–Pt/Al_2O_3 catalysts under the same condition as in situ XAFS experiments mentioned above. Concerning HDA, The TOF values which expressed in the number of converted teteraline per an active site determined by CO adsorption were $0.29 \times 10^2 \, h^{-1}$ for Pd–Pt/SiO_2 and $1.22 \times 10^2 \, h^{-1}$ for Pd–Pt/Al_2O_3. Therefore, Pd–Pt/Al_2O_3 showed about four times higher HDA activity. The HDS activity evaluated by DBT conversion was 100% for Pd–Pt/Al_2O_3 and 84% for Pd–Pt/SiO_2. Both catalysts had equally high activity for HDS.

3.2. In situ XAFS analysis of reduction process

The calcined Pd–Pt catalyst was pressed into a pellet, which was 100 mg in weight and 8 mm in diameter and was put in an in situ XAFS cell designed for high temperature and high pressure liquid phase reactions [5]. The catalyst was activated in situ in the cell under a flow of H_2. Fig. 1 shows the change of Fourier transform of EXAFS ($k^3\chi(k)$, where k and $\chi(k)$ indicate a wave number of a scattered photoelectron and a normalized
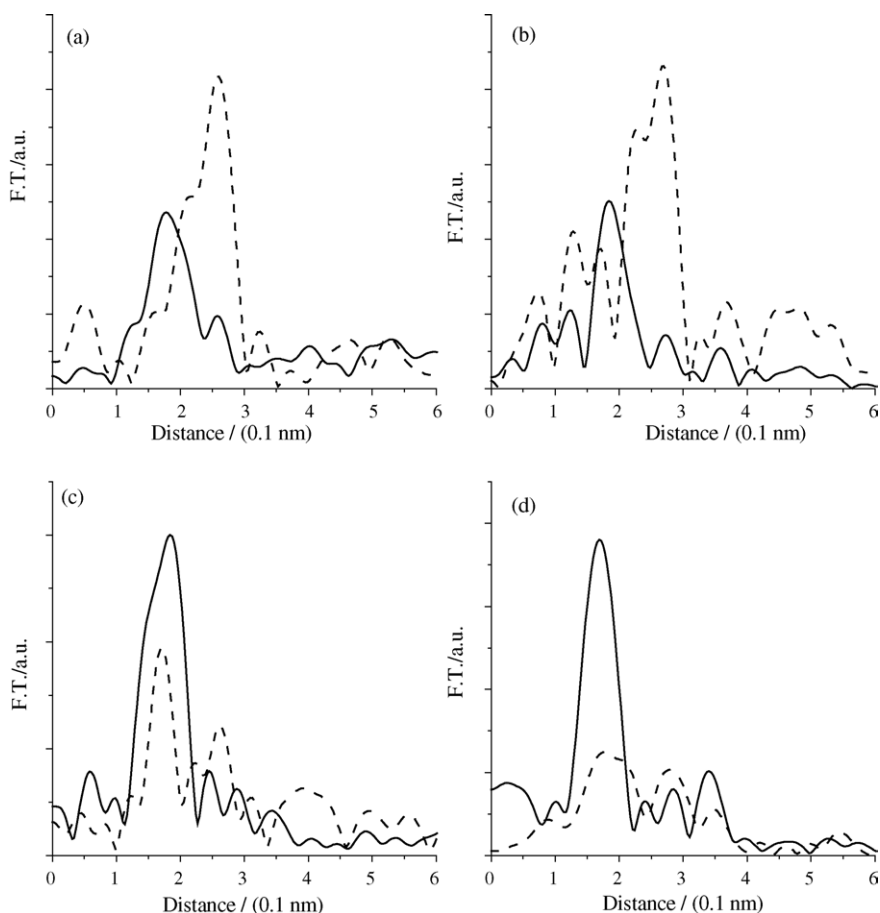

Fig. 1. Fourier transform of EXAFS ($k^3\chi(k)$) spectra observed for catalysts before (solid lines) and after introduction of H_2 at ambient temperature (dotted lines): (a) and (b) are for Pd K-edge and Pt L_{III} edge of Pd–Pt/SiO_2, respectively; (c) and (d) are for Pd K-edge and Pt L_{III} edge of Pd–Pt/Al_2O_3, respectively.

EXAFS oscillation, respectively) spectra observed for catalysts before reduction and after introduction of H_2 at ambient temperature. For the calcined catalysts, there was a peak around 0.16–0.18 nm, which is assigned mainly to metal–oxygen scattering in an oxidized species. For the Pd–Pt/SiO$_2$ (Fig. 1(a) and (b)), the metal–oxygen peak immediately disappeared upon introduction of H_2 to the catalyst and a new peak due to metal–metal scattering emerged at 0.26–0.28 nm and became dominant. On the other hand, for Pd–Pt/Al$_2$O$_3$, contribution of metal–oxygen scattering still remained as a peak at 0.16 nm after introduction of H_2 (Fig. 1(c) and (d)). A metal–metal scattering peak emerged at 0.26 nm, but its intensity was weaker than that of metal–oxygen. Therefore, it is concluded that metal species on SiO$_2$ can be reduced more easily than those on Al$_2$O$_3$ at ambient temperature. It is due to the stronger interaction between metal atoms and Al$_2$O$_3$, compared with SiO$_2$.

Subsequently, the temperature was raised from ambient temperature to 573 K under a flow of H_2. During this process, the change of XANES spectra was recorded as shown in Fig. 2. For the calcined Pd–Pt/SiO$_2$, the Pd K-edge XANES had a peak at 24,360 eV and after introduction of H_2, the peak at 24,360 eV immediately spit into two peaks at 24,345 and 24,380 eV (Fig. 2(a)). The spectrum did not make any noticeable change

Table 1
Coordination numbers (CN) and interatomic distances (R) obtained by curve-fitting analysis of Pd K-edge and Pt L$_{III}$ edge in situ EXAFS spectra observed for the catalysts after reduction at 573 K for 3 h

Sample	Pd K-edge				Pt L$_{III}$ edge			
	Pd–Pd		Pd–Pt		Pt–Pd		Pt–Pt	
	CN	R (nm)	CN	R (nm)	CN	R (nm)	CN	R (nm)
Pd–Pt/SiO$_2$	7.2	0.274	2.5	0.276	9.7	0.273	2.9	0.269
Pd–Pt/Al$_2$O$_3$	7.7	0.273	1.6	0.279	6.0	0.276	2.2	0.269

up to 573 K, which means that reduction of Pd atoms was mostly completed at ambient temperature (Fig. 2(a)) [6]. The XANES spectrum of the Pt atoms on SiO$_2$ also showed a drastic change at ambient temperature (Fig. 2(b)) and like the Pd case, most of the Pt atoms were reduced at this moment. At higher temperature, the Pt L$_{III}$ edge XANES spectra still showed some change. It is due to the change in environment around Pt. The coordination number (CN) of Pt–Pd scattering was 8.2 at ambient temperature (not shown in Table 1) and it increased to 9.7 at 573 K as shown in Table 1. The increase in CN(Pt–Pd) suggests dissolution of Pt atoms into Pd metal particles with temperature. For Pd–Pt/Al$_2$O$_3$, spectral change of XANES due to reduction at ambient temperature can be observed (Fig. 2(c)
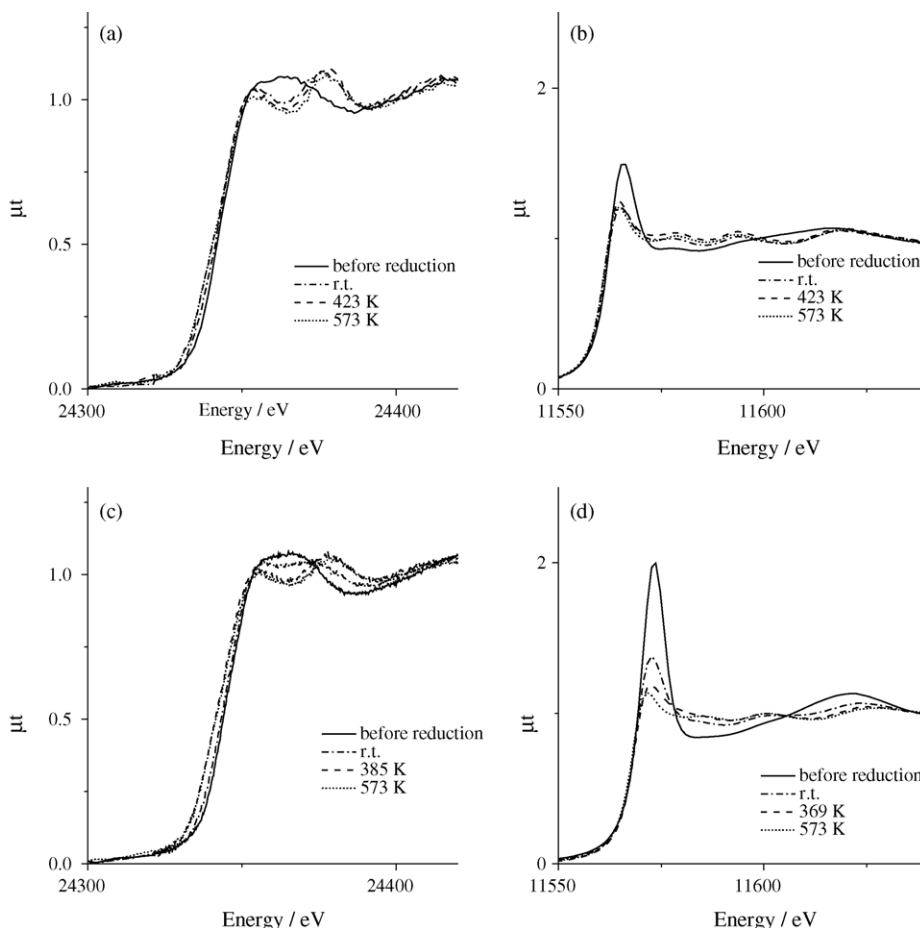

Fig. 2. Change of XANES spectra during reduction process: (a) and (b) are for Pd K-edge and Pt L$_{III}$ edge of Pd–Pt/SiO$_2$, respectively; (c) and (d) are for Pd K-edge and Pt L$_{III}$ edge of Pd–Pt/Al$_2$O$_3$, respectively.

and (d)), which is consistent with the FT results mentioned before. However, reduction of the metal species was not completed at ambient temperature. Judging from the XANES spectra, reduction was almost completed at 385 K for Pd atoms (Fig. 2(c)) and at 369 K for Pt atoms (Fig. 2(d)). In our previous study, where reduction of Pd–Pt/Al$_2$O$_3$ was performed under 20% H$_2$/He and temperature was increased stepwise by 50 K, it was also confirmed that the metal–O scattering band in FT spectra disappeared at 373 K for both Pd K-edge and Pt L$_{III}$ edge [4]. At higher temperature than 369 K, there was still some gradual change in Pt L$_{III}$ edge XANES (Fig. 2(d)). Like in the case of Pd–Pt/SiO$_2$, during further reduction, Pt atoms were gradually dissolved into Pd particles [4].

Table 1 shows the coordination numbers and interatomic distances obtained by curve-fitting analysis of EXAFS for the catalysts after reduction at 573 K. The average coordination numbers of metal–metal scattering (CN(M–M) = (CN(Pd–Pd) + CN(Pd–Pt)) × 4/5 + (CN(Pt–Pd) + CN(Pt–Pt)) × 1/5) was 10.3 for Pd–Pt/SiO$_2$ and 9.1 for Pd–Pt/Al$_2$O$_3$ and that means Pd–Pt/SiO$_2$ had larger metal particles than Pd–Pt/Al$_2$O$_3$, which is supported by dispersion determined by CO adsorption [3]. The coordination number of Pt–Pd for the SiO$_2$ supported catalyst is larger than that of Al$_2$O$_3$ supported one, which indicates that more number of Pd atoms were located around one Pt atom and that results in formation of more uniform Pd–Pt alloy particles on SiO$_2$ compared with Al$_2$O$_3$.

3.3. HDS reaction

After reduction, the HDS of the model oil was conducted at 553 K. Fig. 3 shows FT and XANES spectra of Pd K-edge XAFS observed for Pd–Pt/Al$_2$O$_3$ during the reaction. After reduction, only metal–metal scattering peaks were observed in the range of 0.16–0.25 nm, but after the reaction for 15 min, an intense peak emerged at 0.19 nm and became dominant after 98 min of the reaction. The emerging peak is assigned to metal–sulfur scattering and hence, sulfidation of Pd is confirmed (Fig. 3(a)). In addition to the metal–sulfur peak at 0.19 nm in FT spectra, XANES spectra also showed a change due to sulfidation at 15 min of the reaction, that is, two peaks at 24,356 and 24,379 eV which appeared in the spectrum of a reduced sample merged into one peak at 24,374 eV (Fig. 3(b)). Afterwards, the XANES spectra did not make any noticeable change until 24 h. The change in FT and XANES indicated that modification of electronic state of Pd was completed at 15 min, but further accumulation of sulfur on Pd still proceeded. Judging from the FT spectra, the accumulation of sulfur was saturated at 98 min. According to the catalytic test, there was a serious deactivation of HDA in the initial 1.5 h of the reaction and then the reaction came into steady state. The results of XAFS and the catalytic test are in good agreement with each other, that is, initial rapid sulfidation of metallic sites observed by XAFS well corresponded with the deactivation observed by the catalytic test. Therefore, it is directly confirmed by in situ XAFS that the sulfidation of metallic species was responsible for the initial deactivation. In spite of the initial deactivation, the catalyst still maintained relatively high HDA activity at the steady state. The
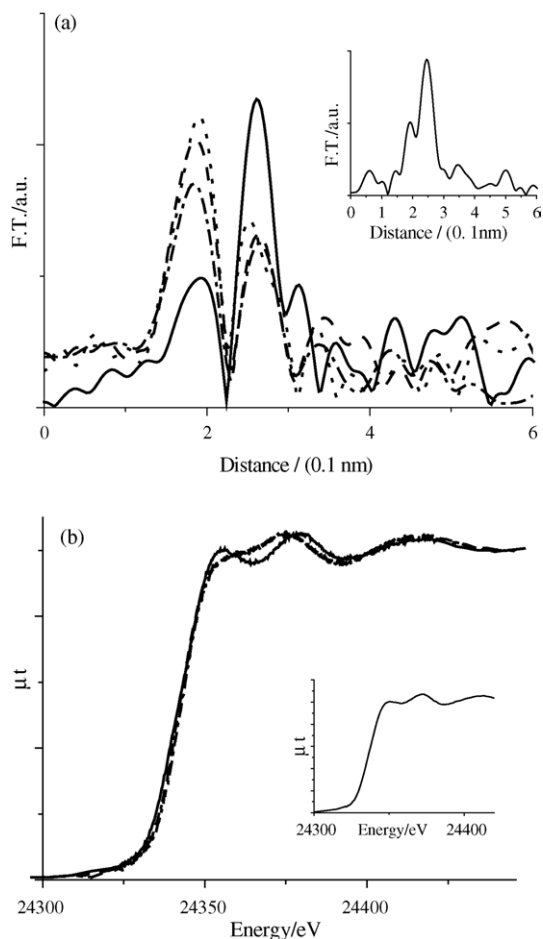

Fig. 3. Change of (a) Fourier transform of Pd K-edge EXAFS and (b) Pd K-edge XANES spectra under HDS conditions observed for Pd–Pt/Al$_2$O$_3$: — before the reaction; — · — · — after 15 min of HDS, – – – 98 min; · · · 24 h. The inset figures were observed after sulfidation of the catalyst at 553 K under a flow of mixed gas composed of 100 ppm H$_2$S, 20% H$_2$ and He for 6 h.

structural analysis of the catalyst in steady state (after 24 h of the reaction) was carried out by EXAFS to determine the structure of active phase. The curve-fitting analysis gave 3.7 for CN(Pd–Pd) and 2.2 for CN(Pd–S), indicating the presence of both sulfided and metallic phases in Pd particles. Since it was technically difficult to carry out the XAFS experiments of HDS catalysts under high pressure and high temperature liquid phase HDS reaction conditions, structural analysis during gas phase sulfidatoin by H$_2$S has been mainly studied to determine the structure of active phase for HDS [7–9]. In our previous work, we also carried out gas phase sulfidation experiments for the same catalysts as a model reaction of HDS [4]. In order to reproduce the similar experimental conditions to that of HDS, the ratio of sulfur/H$_2$ was kept at the same value as HDS in the gas phase experiments. As shown in the inset figure of Fig. 3(a), even after gas phase sulfidation treatment, the metal–metal scattering peaks were still dominant in the FT spectrum and the XANES spectrum also kept a characteristic shape of metal clusters, which had two distinct peaks in the range from 24,300 to 24,400 eV (the inset figure of Fig. 3(b)). That means Pd atoms in Pd–Pt/Al$_2$O$_3$ could resist sulfidation by gas phase H$_2$S. Since, sulfidation of Pd atoms was immediately observed under HDS conditions, the effect of
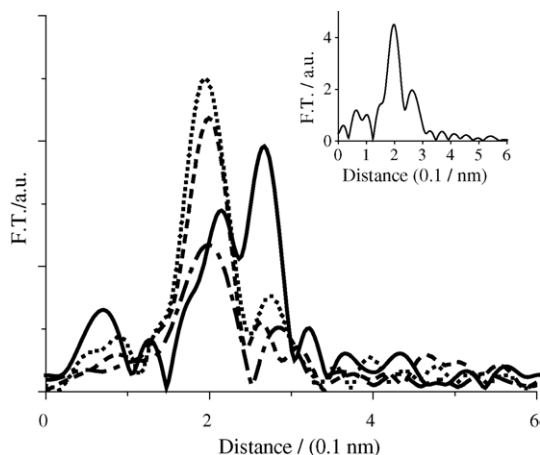
Fig. 4. Fourier transform of Pt L_{III} edge EXAFS under HDS conditions observed for Pd–Pt/Al$_2$O$_3$: — before the reaction; — • — • — after 2 min of HDS; – – – 101 min; ⋯ 24 h. The inset figure was observed after sulfidation of the catalyst at 553 K under a flow of mixed gas composed of 100 ppm H$_2$S, 20% H$_2$ and He for 6 h.

Table 2
Coordination numbers obtained by curve-fitting analysis of Pd K-edge and Pt L_{III} edge in situ EXAFS spectra observed for the catalysts after HDS for 24 h

Sample	Pd K-edge			Pt L_{III} edge		
	Pd–Pd	Pd–Pt	Pd–S	Pt–Pd	Pt–Pt	Pt–S
Pd–Pt/SiO$_2$	6.1	3.4	–	6.5	3.7	–
Pd–Pt/Al$_2$O$_3$	3.7	–	2.2	2.2	–	5.9

sulfur in HDS is supposed to be different from that of gas phase conditions. And also the structure of the Pd atoms under gas phase sulfidation conditions was suggested to be different from that under HDS conditions. On the other hand, the contribution of metal–sulfur scattering was clearly observed in FT spectra of Pt L_{III} edge EXAFS as an intense peak at 0.19 nm for both HDS and gas phase reactions (Fig. 4). However, the structure around the Pt atoms was not the same. For the catalyst after HDS, the CN(Pt–S) and CN(Pt–Pd) were 5.9 and 2.2, respectively (Table 2), whereas, CN(Pt–S) was 4.2 and CN(Pt–Pd) was 3.9 after gas phase sulfidation [4]. Lager CN(Pt–S) and smaller CN(Pt–Pd) for HDS, compared with the gas phase reaction, indicate that deeper sulfidation of Pt occurred under HDS. In addition to that, judging from the CN of Pd–S and Pt–S (Table 2), the average degree of sulfidation of Pt was larger than that of Pd. So it is suggested that Pt atoms were located more sulfur-accessible positions than Pd atoms and such positions were probably near the outer surface of metal clusters.

For Pd–Pt/SiO$_2$, the contribution of metal–sulfur scattering could not be find in FT of either Pd K-edge or Pt L_{III} edge EXAFS until the end of the reaction (Fig. 5(a) and (c)). This is also confirmed by XANES spectra (Fig. 5(b) and (d)), that is, two peaks characteristic of metal clusters could be observed at 24,360 and 24,370 eV in Pd K-edge XANES and for Pt L_{III} edge XANES, no noticeable change was observed during all the period of the reaction. However, according to the catalytic test, the HDA activity decayed to 1/10 during the initial 5 h and then reached a steady state. This serious deactivation of HDA in the presence of sulfur strongly suggests the formation of sulfide
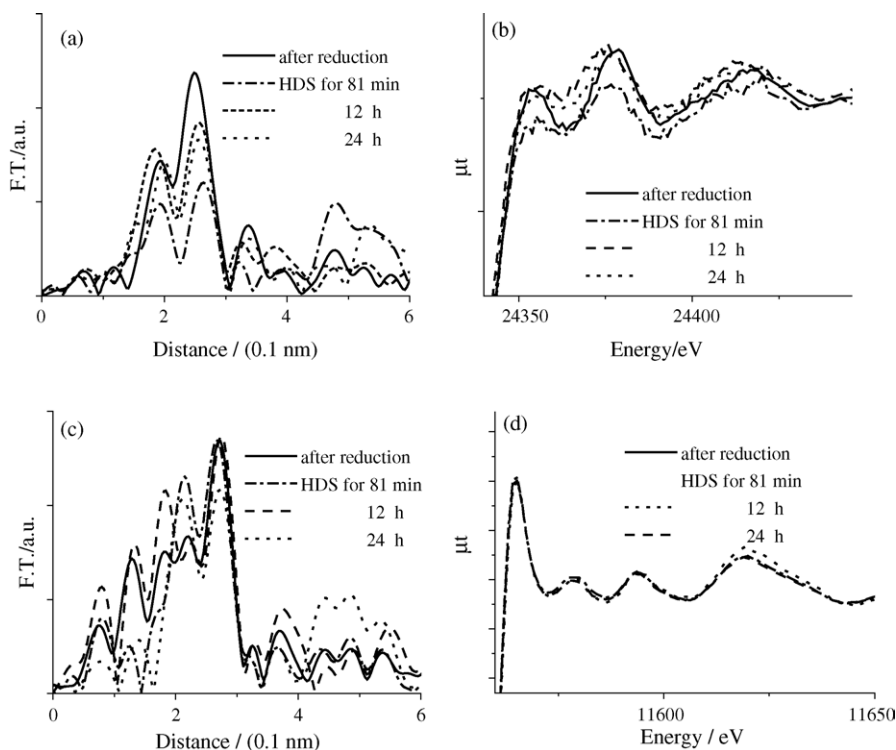

Fig. 5. Change of Fourier transform of EXAFS and XANES spectra during HDS observed for Pd–Pt/SiO$_2$: (a) and (b) are Fourier transform of Pd K-edge EXAFS and XANES, respectively; (c) and (d) are Fourier transform of Pt L_{III} edge EXAFS and XANES, respectively.

phase on the surface of metal particles, even though no direct evidence of sulfur was obtained by XAFS analysis.

Regarding HDS, both Pd–Pt/SiO$_2$ and Pd–Pt/Al$_2$O$_3$ showed high activity. The active sites of supported metal catalysts for HDS are generally composed of surface sulfided species. So, it is suggested that both catalysts have some sulfided species on the surface. The presence of sulfided phase was confirmed for Pd–Pt/Al$_2$O$_3$, but no evidence of sulfur was obtained in XAFS analysis for Pd–Pt/SiO$_2$. For Pd–Pt/SiO$_2$, if a very thin sulfide layer covered all the surface of the metal particles, the CN(metal–sulfur) could be less than 1. But the contribution of such sulfur component could be hidden in the intense EXAFS oscillation of metal–metal scattering, whose CN(metal–metal) is about 10 (CN(Pd–Pd) + CN(Pd–Pt) = 9.5 or CN(Pt–Pd) + CN(Pt–Pt) = 10.2 for Pd–Pt/SiO$_2$) in total (Table 2). Compared with Pd–Pt/Al$_2$O$_3$, Pd–Pt/SiO$_2$ showed much lower HDA activity, even though most of the metal species remained in a metallic state. It could be well understood if the surface of the metallic particles on Pd–Pt/SiO$_2$ was mostly covered with a thin sulfide layer which was inactive for HDA. The sulfide layer suppressed not only HDA activity, but also further sulfidation of the inner part of the metal particles. In other words, it protected metallic sites from sulfidation. It is reported that formation of Pd–Pt alloy on the catalysts greatly improves the sulfur tolerance of monometallic counterparts [1,2,10]. One of the explanations for high sulfur tolerance of Pd–Pt is that electro-deficient character of Pt suppressed formation of metal–sulfur bonding [1]. In the present study, the Pt atoms in Pd–Pt/SiO$_2$ were uniformly distributed in the alloy particle, therefore, the surface of the metal particles was kept uniformly in an electro-deficient state and had a high resistance against sulfur. Sulfidation was limited only on the surface of metal particles and a thin layer of sulfide was formed, protecting the inner metallic part from further sulfidation.

On the other hand, Pd and Pt atoms on Al$_2$O$_3$ formed a rather segregated structure [4]. Sulfidation of Pd–Pt species proceeded deep inside of the metal particles as soon as HDS started, but metallic sites still existed together with sulfide species on the surface in the steady state. Since, sulfidation degree of Pt is higher than Pd, most of the Pt atoms were rather segregated and located at more sulfur-accessible sites, namely, on the outer surface of the catalyst. But there were also some metallic sites on the surface, which worked as an HDA reaction center. That is a similar situation as reported in the literature [1]. Regarding a sulfur–tolerant Ru catalysts, similar findings have been reported. That is, a zeolite supported Ru catalyst was a sulfur–tolerant catalyst for HDA and the active phase of the catalyst consisted of Ru sulfide phase and very small domains of Ru metal [11].

It is concluded that the structure of the active phase of Pd–Pt catalysts deeply depended on the nature of the support and the partially sulfided surface structure was the active phase for HDA reactions in the presence of sulfur.

4. Conclusions

The in situ XAFS analysis of Pd–Pt/SiO$_2$ and Pd–Pt/Al$_2$O$_3$ under HDS conditions was carried out. The two catalysts showed the same HDS activity, but regarding HDA, Pd–Pt/Al$_2$O$_3$ showed higher activity. The structural analysis of before and during the reaction showed that Pd–Pt/SiO$_2$ had relatively uniform metallic alloy particles and only the metallic phase could be found by XAFS during the reaction. However, probably due to the presence of a thin sulfide layer on the surface, which covered the active sites for HDA reaction, the HDA activity was suppressed. On the other hand, metal species on Pd–Pt/Al$_2$O$_3$ formed rather segregated structure and were subjected to more serious sulfidation during the reaction. But the presence of both metallic and sulfide phases on the surface kept the HDA activity high under HDS conditions. It is concluded that partially sulfided phase on the surface is closely related to the catalytic activity.

References

[1] R.M. Navarro, B. Pawelec, J.M. Trejo, R. Mariscal, J.L.G. Fierro, J. Catal. 189 (2000) 184.
[2] H. Yasuda, Y. Yoshimura, Catal. Lett. 46 (1997) 43.
[3] H. Yasuda, T. Kameoka, T. Sato, N. Kijima, Y. Yoshimura, Appl. Catal. A: Gen. 185 (1999) L199.
[4] K.K. Bando, T. Matsui, Y. Ichihashi, K. Sato, T. Tanaka, M. Imamura, N. Matsubayashi, Y. Yoshimura, Phys. Scr. T115 (2005) 828.
[5] T. Kawai, K.K. Bando, Y.-K. Lee, S.T. Oyama, W.-J. Chun, K. Asakura, Chem. Lett., in preparation.
[6] K.K. Bando, L. Le Bihan, H. Yasuda, K. Sato, T. Tanaka, F. Dumeignil, M. Imamura, N. Matsubayashi, Y. Yoshimura, Anal. Sci. 17 (2001) i127.
[7] G.U. Kulkarni, C.N.R. Rao, Catal. Lett. 9 (1991) 427.
[8] R. Cattaneo, T. Weber, T. Shido, R. Prince, J. Catal. 191 (2000) 225.
[9] T. Kubota, N. Hosomi, K.K. Bando, T. Matsui, Y. Okamoto, Phys. Chem. Chem. Phys. 5 (2003) 4510.
[10] T. Fujikawa, K. Tsuji, H. Mizoguchi, H. Godo, K. Idei, K. Usui, Catal. Lett. 63 (1999) 27.
[11] B. Moraweck, G. Bergeret, M. Cattenot, V. Kougionas, C. Geantet, J.-L. Portefaix, J.L. Zotin, M. Breysse, J. Catal. 165 (1997) 45.